Pressure-Responsive Polymer Chemosensors for Hydrostatic Pressure-Signal Detection: Poly-L-Lysine-Pyrene Conjugates

Soshi Wakako, Yumiko Hori, Tomokazu Kinoshita, Takao Saiki, Xinyi Qi, Koki Hasegawa, Yoshitane Imai, Tadashi Mori, Keiichi Nakagawa, and Gaku Fukuhara*

ABSTRACT: Stimulus-responsive polymer materials are an attractive alternative to conventional supramolecular and polymer assemblies for applications in sensing, imaging, and drug-delivery systems. Herein, we synthesized a series of pyrene-labeled α- and ε-poly-L-lysine conjugates with varying degrees of substitution (DSs). Hydrostatic pressure-UV/vis, fluorescence, excitation spectroscopies, and fluorescence lifetime measurements revealed ground-state conformers and excited-state ensembles emitting fluorescence with variable intensities. The polylysine-based chemosensors demonstrated diverse ratiometric responses to hydrostatic pressure through adjustments in polar solvents, DSs, and polymer backbones. Additionally, the fluorescence chemosensor exhibited a promising g_{lum} value of 3.2×10^{-3}, indicating potential applications in chiral fluorescent materials. This study offers valuable insights for the development of smart hydrostatic pressure-responsive polymer materials.

Chemosensors, also known as chemical and synthetic probes, exhibit notable optical signals such as colorimetric, fluorometric, and electrochemical responses when subjected to variations in temperature, pH, pressure, and mechanochemical properties (such as tension and stress).[1–7] Notably, chemosensors that demonstrate selectivity and sensitivity in their signals are more suitable for ratiometric signal-readout systems than simple on/off signaling.[8–13] Ratiometric sensing/imaging approaches offer advantages in terms of reducing background noises and signal interferences, making them particularly superior in these aspects.[14–17] For example, biological systems often employ the fluorescence resonance energy transfer (FRET) mechanism, where fluorescence responses in donor and acceptor chromophores mutually change.[18–20] Therefore, developing functional ratiometric signaling systems poses a significant challenge in multidisciplinary chemistry.[8–20]

In recent years, there has been significant progress in the synthesis of dynamically controllable chemosensors and smart materials that respond to external stimuli such as temperature, pressure, chemical additives, and photoirradiation.[21–24] In particular, hydrostatic pressure has gained attention in the field of "mechano" science,[21] including mechanochemistry[25–27] and mechanobiology.[5–7, 28–30] Although the effects of hydrostatic pressure in the solution state have been studied since the 1960s,[31–46] this excludes high-pressure solid chemistry using diamond anvil cells.[47,48] Indeed, we have successively developed the hydrostatic pressure-control concept by inducing pressure-responsive (chir)optical changes on the functional materials.[21] Among these advancements, notable examples include the mechanochromophore in thermally activated delayed fluorescence (TADF)[49] and the dynamic polymers in aggregation-induced emission (AIE),[50] both of which exhibit ratiometric responses under the influence of hydrostatic pressure. These discoveries have motivated us to develop a practical ratiometric chemosensor that can be controlled by hydrostatic pressure.

In this study, we discovered functional polymer chemosensors that can exhibit ratiometric hydrostatic pressure signaling. The conceptual scheme, as depicted in Figure 1a, involves the application of hydrostatic pressure to induce conformational changes in the polymer, resulting in perturbations in the fluorescence intensities of the monomer and excimer forms as ratiometric responses. The choice of pyrene as a fluorophore in the polymer design is crucial owing to its dual emissive behavior as a monomer and an excimer. For the dynamic polymer scaffold, we selected α-poly-L-lysine (**α-PLL**) and ε-poly-L-lysine (**ε-PLL**), with the difference in the number of methylene groups expected to play a significant role in the dynamics of the polymer backbones. The molecular design is greatly inspired by the fluorescence data of the pyrene-labeled PLLs[51] and other flexible polymers[52,53] under atmospheric conditions (0.1 MPa). Moreover, the degree of substitution (DS) of pyr on the polymer backbone is highly likely to significantly impact ratiometric signaling. Hence, we synthesized a series of varying DSs (low, middle, or high DS) of **α-PLLpyr** and **ε-PLLpyr** conjugates, respectively, and **pyr-ref** as the reference monomer, as shown in Figure 1b. Herein, we present the ratiometric responses observed upon hydrostatic pressurization using **α-PLLpyr** and **ε-PLLpyr** in different solvents, including MeOH, H_2O, and PBS. The choice of PBS solution, which closely resembles the biological medium with an ionic strength of 166 mM, allows for potential applications of these polymer chemosensors in biocompatible materials. By conducting comparative studies in both hydrophilic organic solvents and aqueous solutions, we aim to gain deeper mechanistic insights into the factors influencing the ratiometric signaling behavior of the polymer chemosensors. These insights may eventually pave the way for applications in mechanobiological imaging.

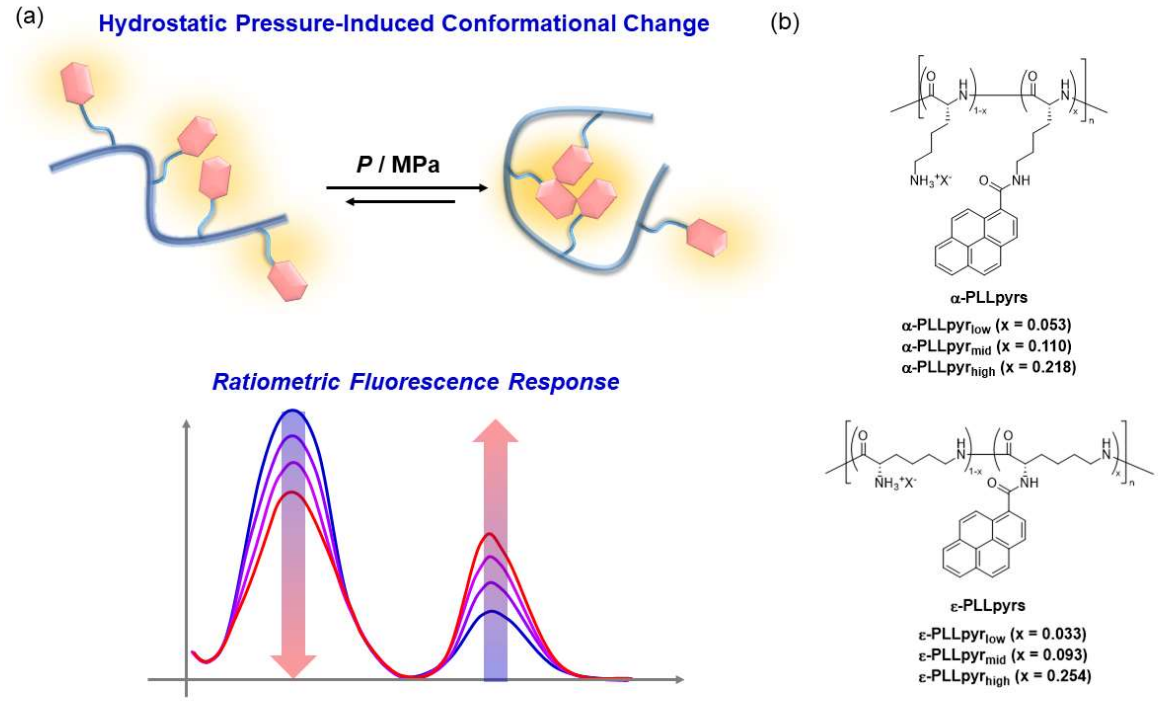

Figure 1. (a) Schematic illustrations of the concept for the ratiometric fluorescence signaling based on the hydrostatic pressure-induced conformational changes of polymer chemosensors. (b) Chemical structures of the polymer chemosensors (**α- and ε-PLLpyrs**) and the reference compound **pyr-ref**.

First, we investigated the ratiometric behaviors (the monomer/excimer ratio) of all the polymers at 0.1 MPa (atmospheric pressure). As shown in Figures 2a and b, both α- and **ε-PLLpyrs** showed a sudden increase in excimer emission at 500 nm with increasing DS in DMSO; naturally, the monomeric reference **pyr-ref** exhibited no excimer emission. This is attributed to the degree of crowding of **pyr** chromophores on the polymer backbones. Therefore, we will further investigate the effect of hydrostatic pressurization on these ratiometric responses, particularly in PBS.

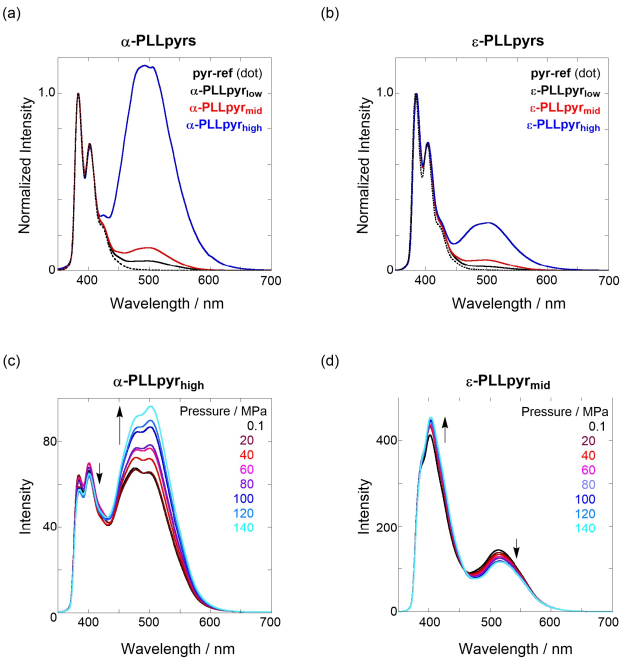

Figure 2. (a,b) Normalized fluorescence spectra of DMSO solutions of (a) **α-PLLpyrs** (20-27 μM) and (b) **ε-PLLpyrs** (17-25 μM) with **pyr-ref** (16 μM, dotted), measured at 25 °C in a 1-cm cell. (c,d) Fluorescence spectra of (c) **α-PLLpyr$_{high}$** (37 μM) and (d) **ε-PLLpyr$_{mid}$** (33 μM) in PBS at 0.1, 20, 40, 60, 80, 100, 120, and 140 MPa (from black to sky blue) at room temperature in a high-pressure cell. Polymer concentrations were expressed in the chromophore unit.

As a representative ratiometric polymer, **α-PLLpyr$_{\mathbf{high}}$** in PBS (Figure 2c) was first examined. Importantly, under hydrostatic pressurization, the monomer emission intensity slightly decreased while the excimer intensity increased. This simple ratiometric response provides a means for detecting applied hydrostatic pressures. In contrast, as shown in Figures S20a and b in the SI, both **α-PLLpyr$_{\mathbf{low}}$** and **α-PLLpyr$_{\mathbf{mid}}$** exhibited a mutual decrease in both monomer and excimer intensities with increasing hydrostatic pressure. The degrees of decrease varied in each polymer, resulting in inherent ratiometric characteristics, as shown in Table 2. Furthermore, the hydrostatic pressure-dependent fluorescence changes of **α-PLLpyrs** (and **ε-PLLpyrs**) in MeOH and H_2O are presented in Figures S21–S24 in the SI. The observed changes in intensity ratios (monomer/excimer ratios) varied depending on the solvents and chromophore substitution (DSs) used, indicating that ratiometric signaling under hydrostatic pressurization can be controlled by various parameters.

To elucidate the excited-state species involved in **α-PLLpyrs** in more detail, we measured the fluorescence lifetimes in PBS upon hydrostatic pressurization. In Figure 3a,b, the fluorescence decay profile at 400 nm (around the monomer) or 500 nm (around the excimer) in PBS exhibited multiple components and could be fitted reasonably well with a sum of three exponential functions (fitting results shown in Figure S25). Interestingly, in the monomer emissive region, we observed three distinct excited species with lifetimes of 0.2 ns (τ_1), 9.1 ns (τ_2), and 27 ns (τ_3) at atmospheric pressure (0.1 MPa), as listed in Table 1. Comparing with **pyr-ref**, the longest τ_3 species was attributed to the pyrene monomeric species. The shortest species of 0.2 ns was also observed in **pyr-ref**, and its origin was not previously concluded in the literature for similar chromophores.[54] This short lifetime may be explained by a proton transfer involving the NH group in the amide moiety. Additionally, the middle species with a lifetime of τ_2 can be attributed to the ground-state stacked conformer (GSC), which generally exhibits a shorter lifetime compared to the monomeric species, as reported in our previous study.[55] This observation is further supported by the hydrostatic pressure-excitation spectra, which do not overlap with the UV/vis spectrum (refer to Figure S26 in the SI). Based on these findings, we can identify the ground-state conformers and excited-state species on the polymer backbone, as shown in Figure 3c. Increasing hydrostatic pressure results in shortened lifetimes and decreasing relative abundances (*A* factors) of the main monomer emissive species, leading to a decrease in fluorescence intensity in the monomer emission region. This behavior is likely attributed to the flexibility of the polymer backbone. A detailed discussion on this aspect will be provided later by comparing with **ε-PLLpyrs.** Similarly, three lifetimes of 4.2 (τ_4), 24 (τ_5), and 54 ns (τ_6) were observed in the excimer region at 0.1 MPa; however, their origin was unclear. The most plausible explanation for τ_4 is that it may correspond to a different type of ground-state stacked conformation (GSC). In this GSC2, the pyr stacking energy is more stable than in GSC1, resulting in emission at a longer wavelength. Similarly to pyr chromophores in a polymer matrix,[56] the two longer lifetimes, τ_5 and τ_6, can be attributed to a second (partially overlapped) excimer and a sandwich (fully overlapped) excimer, respectively. Applying hydrostatic pressure leads to an increase in the *A* factor of the sandwich excimer. These observations in fluorescence lifetime measurements are the underlying cause of the hydrostatic pressure-induced ratiometric responses in the polymer chemosensor.

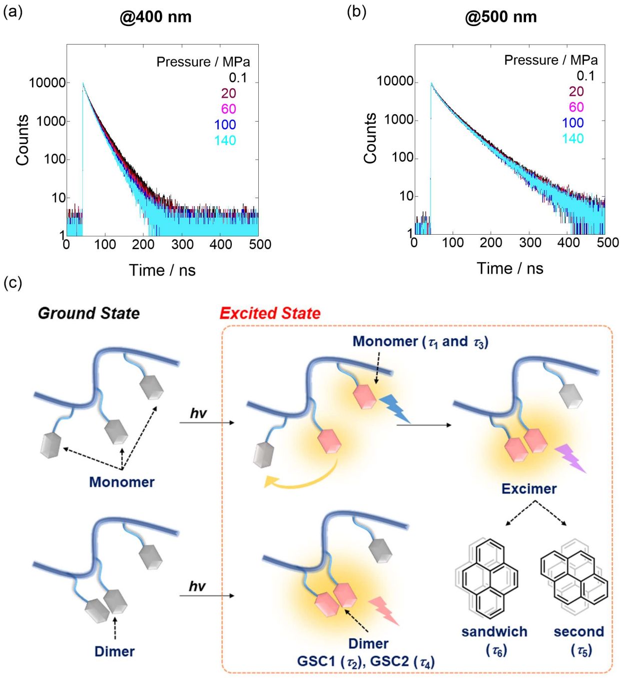

Figure 3. (a,b) Time-correlated fluorescence decays of **α-PLLpyr$_{\mathbf{high}}$** (37 μM) monitored at (a) 400 nm and (b) 500 nm in PBS at 0.1, 20, 60, 100, and 140 MPa (from black to sky blue) at room temperature in a high-pressure cell. Polymer concentrations were expressed in chromophore units. (c) Schematic illustration of the ground-state conformers and excited-state dynamics for the hydrostatic pressure-induced ratiometric responses of the chemosensors.

Table 1. Fluorescence Lifetimes of α-PLLpyr$_{\text{high}}$ in PBS[a]

Compd.	P/MPa	λ_{em}[b]/nm	n[c]	τ_1/ns	A_1	τ_2/ns	A_2	τ_3/ns	A_3	τ_4/ns	A_4	τ_5/ns	A_5	τ_6/ns	A_6	χ^2
pyr-ref[d]	0.1	400	2	0.2	<0.01			14	0.99							1.3
α-PLLpyr$_{\text{high}}$	0.1	400	3	0.2	0.02	9.1	0.22	27	0.76							1.2
		500	3							4.2	0.04	24	0.31	54	0.65	1.1
	20	400	3	0.2	0.02	9.2	0.24	25	0.74							1.3
		500	3							4.5	0.04	25	0.35	54	0.61	1.1
	60	400	3	0.2	0.02	8.9	0.25	24	0.73							1.0
		500	3							4.1	0.04	23	0.34	53	0.62	1.0
	100	400	3	0.2	0.02	8.5	0.25	23	0.73							1.1
		500	3							4.1	0.04	24	0.35	50	0.61	1.2
	140	400	3	0.2	0.02	8.2	0.25	22	0.73							1.0
		500	3							3.1	0.03	19	0.25	49	0.72	1.1

[a]Fluoresecence lifetime (τ_i/ns) and relative abundance (A_i) of each excited species in non-degassed PBS at room temperature in a high-pressure cell; [**α-PLLpyr$_{\text{high}}$**] = 37 μM in chromophore unit. [b]Monitoring wavelength. [c]Number of components. [d][**pyr-ref**] = 33 μM, measured in MeOH.

Next, we investigated the hydrostatic pressure signaling of **ε-PLLpyrs**, in which the polymer backbone is believed to be more susceptible to a hydrostatic pressure stimulus owing to the flexible methylene chain in the repeating unit. Figure 2b demonstrates that increasing the DS results in the stepwise development of excimer emission in DMSO, similar to the behavior observed in **α-PLLpyrs**. However, the excimer emission of **ε-PLLpyr$_{\text{high}}$** in PBS shows a slightly distorted spectral shape (see Figure S20d). This distortion may be attributed to the presence of aggregated patterns in the excited state, which are plausible in hydrophilic and high-ionic-strength solutions such as PBS owing to the flexible chain. Notably, **ε-PLLpyr$_{\text{mid}}$** exhibits remarkable ratiometric signaling upon hydrostatic pressurization in Figure 2d, with the monomer emission intensity increasing and the excimer emission intensity decreasing with increasing pressure. Interestingly, this behavior is opposite to **α-PLLpyr$_{\text{high}}$**. To elucidate the excited-state dynamics of **ε-PLLpyr$_{\text{mid}}$**, the hydrostatic pressure lifetime decay was measured. The fluorescence decay profiles measured at 400 (monomer region) and 500 (excimer region) nm were reasonably fitted to give a sum of three functions (see Figure S27 and Table S1 in SI). These six excited species correspond to τ_1 and τ_3 originating from the pyr chromophore, τ_2 and τ_4 as GSC1 and GSC2, τ_5 as the second excimer, and τ_6 as the sandwich excimer, respectively. The opposite ratiometry, with decreasing excimer emission and increasing monomer emission, can be attributed to the decreasing A factor of τ_6. While the A factors in the monomer species also decrease, they are not the main determining factor for the increase in fluorescence intensity. Generally, the fluorescence intensity increases with increasing hydrostatic pressure owing to the increasing viscosity of the solution, suppressing collisional deactivation by a solvent attack.[21,46] In the monomer region, this mechanism is preferable, eventually leading to an increase in intensity.

Table 2 summarizes the hydrostatic pressure-ratiometric responses (see Figure S28). The response factors γ (the fluorescence intensity ratios of monomer/excimer) in MeOH, a hydrophilic but organic solvent, are larger than those obtained in aqueous solutions such as H_2O and PBS. These different behaviors are likely to be responsible for the conformational changes of the polymer backbones. As shown in the circular dichroism (CD) spectra of Figure S29a, **α-PLL** in MeOH shows two characteristic Cotton peaks relating to α-helix and β-sheet; in contrast, the CD spectra of the aqueous solutions show only negative maxima (Figure S29b,c). These results and previous studies[57] suggest that **α-PLL** adopts a higher-ordered structure in MeOH but a random coil conformation in aqueous solution. Furthermore, the pressure-dependent viscosity of MeOH exhibits a significant change, increasing from 0.544 cP at 0.1 MPa to 0.924 cP at 151 MPa.[58] Conversely, H_2O's pressure-dependent viscosity shows little change, ranging from 0.890 cP to 0.889 cP over a pressure range of 0.1 MPa to 100 MPa.[59] Solution viscosity is crucial for the ground- and excited-state dynamics of chromophores. Therefore, we revealed that these two factors are critical in generating larger γ values compared to those obtained in aqueous solutions. Additionally, the CD spectra of **ε-PLL** in all the studied solvents (as shown in Figure S29d-f) exhibited broad positive Cotton effects, indicating an extended conformation.[60] The conformational flexibility of **ε-PLLpyrs**, which is attributed to the methylene linkers in the repeating unit, results in higher γ values compared to **α-PLLpyrs**. This suggests that **ε-PLLpyrs** exhibit better performance as hydrostatic pressure-ratiometric signaling chemosensors.

Table 2. Hydrostatic Pressure-Induced Ratiometric Responses

Chemosensor	Response factor (γ) /$\lvert\times10^{-3}$ MPa$^{-1}\rvert^{b}$		
	in MeOH	in H_2O	in PBS
α-PLLpyr$_{\mathbf{low}}$	16	2.7	2.0
α-PLLpyr$_{\mathbf{mid}}$	8.2	2.0	1.5
α-PLLpyr$_{\mathbf{high}}$	6.6	2.1	4.0^{c}
ε-PLLpyr$_{\mathbf{low}}$	47	15	13
ε-PLLpyr$_{\mathbf{mid}}$	20	2.7	8.2
ε-PLLpyr$_{\mathbf{high}}$	5.9	2.0	*a*

^{a}Not applicable. $^{b}I_{\mathrm{monomer}}/I_{\mathrm{excimer}}$, unless noted otherwise. $^{c}I_{\mathrm{excimer}}/I_{\mathrm{monomer}}$.

Finally, we investigated the circularly polarized luminescence (CPL) emitted by the pyrene-based polymer chemosensors to explore their potential as chiral emitters. Figure 4 shows that **ε-PLLpyr$_{\mathbf{high}}$** exhibited negative CPL in the excimer regions, with a g_{lum} of 2.1 × 10^{-3} in MeOH and 3.2 × 10^{-3} in H_2O, respectively. These values are slightly larger than those observed in the chirally modified pyrenic chromophores ($<10^{-3}$).[61,62] This phenomenon can be attributed to the close packing of pyrene chromophores on the chiral PLL backbone. The g_{lum} value, as defined in Equation 1, allows us to quantitatively describe the circularly polarized luminescence as:

$$\frac{I_L}{I_R} = \frac{\left(1+\frac{glum}{2}\right)}{\left(1-\frac{glum}{2}\right)} \quad (1)$$

The parameter I_L/I_R, representing the ratio of left-handed to right-handed CPL, becomes a chiral ratiometric factor of 1.0021 in MeOH or 1.0032 in H_2O. This new index provides a quantitative measure of the chiral properties of the fluorophore polymer chemosensors.

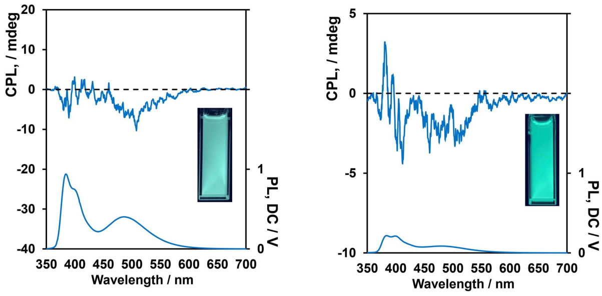

Figure 4. CPL emission (top) and total emission (PL) spectra of **ε-PLLpyr$_{\mathbf{high}}$** in (a) MeOH (46 μM in chromophore unit) and (b) H_2O (46 μM in chromophore unit) at room temperature. The insets show the photographs of the solutions.

In conclusion, this study reports the discovery of ratiometric response polymer chemosensors induced by hydrostatic pressure, representing a novel approach in the field of "mechano" science. These findings provide a precise method for detecting hydrostatic pressures and offer advantages in terms of sensitive and selective signal readout. The use of pressure-responsive polymer chemosensors, especially in a ratiometric manner, holds great promise for various applications. Hence, this study provides guidelines for designing smart polymer materials with ratiometric responses to hydrostatic pressure and notable CPL performance, facilitating the development of advanced multifunctional polymer materials.

ASSOCIATED CONTENT

The Supporting Information is available free of charge via the Internet at http://pubs.acs.org.

Experimental section; synthesis and characterization of the chemosensors; fluorescence and excitation spectra and fluorescence lifetime decays of the chemosensors under hydrostatic pressures; the ratiometric response as a function of hydrostatic pressure; CD spectra of poly-L-lysines.

AUTHOR INFORMATION

Corresponding Author

Gaku Fukuhara – Department of Chemistry, Tokyo Institute of Technology, 2-12-1 Ookayama, Meguro-ku, Tokyo 152-8551, Japan; orchid.org/0000-0002-2189-8943; Email: gaku@chem.titech.ac.jp

Authors

Yumiko Hori – Department of Chemistry, Tokyo Institute of Technology, 2-12-1 Ookayama, Meguro-ku, Tokyo 152-8551, Japan
Tomokazu Kinoshita – Department of Chemistry, Tokyo Institute of Technology, 2-12-1 Ookayama, Meguro-ku, Tokyo 152-8551, Japan
Takao Saiki – Department of Precision Engineering, The University of Tokyo, 7-3-1 Hongo, Bunkyo-ku, Tokyo 113-8656, Japan
Xinyi Qi – Department of Bioengineering, The University of Tokyo, 7-3-1 Hongo, Bunkyo-ku, Tokyo 113-8656, Japan
Koki Hasegawa – Graduate School of Science and Engineering, Kindai University, 3-4-1 Kowakae, Higashi-Osaka, Osaka 577-8502, Japan
Yoshitane Imai – Department of Applied Chemistry, Faculty of Science and Engineering, Kindai University, 3-4-1 Kowakae, Higashi-Osaka, Osaka 577-8502, Japan
Tadashi Mori – Department of Applied Chemistry, Osaka University, 2-1 Yamada-oka, Suita 565-0871, Japan; orchid.org/0000-0003-3918-0873
Keiichi Nakagawa – Department of Precision Engineering, Department of Bioengineering, The University of Tokyo, 7-3-1 Hongo, Bunkyo-ku, Tokyo 113-8656, Japan; orcid.org/0000-0001-6013-0462

Notes

The authors declare no competing financial interest.

ACKNOWLEDGMENT

G.F. appreciates the generous supports provided by Grant-in-Aid (No. 19H02746, 23H04020) from the Japan Society for the Promotion of Science (JSPS). T.M. acknowledges support for this work by Japan Science and Technology (JST), CREST (No. JPMJCR2001). We are grateful to Ms. Kotoe Nakasha, Dr. Sachise Karakawa, and Dr. Daigo Iwahata of Ajinomoto Co., Inc. for their fruitful discussions.

REFERENCES

(1) Shinkai, S.; Ikeda, M.; Sugasaki, A.; Takeuchi, M. Positive Allosteric Systems Designed on Dynamic Supramolecular Scaffolds: Toward Switching and Amplification of Guest Affinity and Selectivity. *Acc. Chem. Res.* **2001**, *34*, 494–503.

(2) You, L.; Zha, D.; Anslyn, E. V. Recent Advances in Supramolecular Analytical Chemistry Using Optical Sensing. *Chem. Rev.* **2015**, *115*, 7840–7892.

(3) Schroeder, V.; Savagatrup, S.; He, M.; Lin, S.; Swager, T. M. Carbon Nanotube Chemical Sensors. *Chem. Rev.* **2019**, *119*, 599–663.

(4) Fukuhara, G. Analytical supramolecular chemistry: Colorimetric and fluorimetric chemosensors. *J. Photochem. Photobiol. C: Photochem. Rev.* **2020**, *42*, 100340.

(5) Chen, J.; Peng, Q.; Peng, X.; Han, L.; Wang, X.; Wang, J.; Zeng, H. Recent Advances in Mechano-Responsive Hydrogels for Biomedical Applications. *ACS Appl. Polym. Mater.* **2020**, *2*, 1092–1107.

(6) Rivera-Tarazona, L. K.; Campbell, Z. T.; Ware, T. H. Stimuli-responsive engineered living materials. *Soft Matter* **2021**, *17*, 785–809.

(7) Hua, B.; Shao, L.; Li, M.; Liang, H.; Huang, F. Macrocycle-Based Solid-State Supramolecular Polymers. *Acc. Chem. Res.* **2022**, *55*, 1025–1034.

(8) McLaurin, E. J.; Bradshaw, L. R.; Gemelin, D. R. Dual-Emitting Nanoscale Temperature Sensors. *Chem. Mater.* **2013**, *25*, 1283–1292.

(9) Lee, M. H.; Kim, J. S.; Sessler, J. L. Small molecule-based ratiometric fluorescence probes for cations, anions, and biomolecules. *Chem. Soc. Rev.* **2015**, *44*, 4185–4191.

(10) Haidekker, M. A.; Theodorakis, E. A. Ratiometric mechanosensitive fluorescent dyes: design and applications. *J. Mater. Chem. C* **2016**, *4*, 2707–2718.

(11) Hawes, C. S.; Gunnlaugsson, T. Multichannel Luminescent Lanthanide Polymers as Ratiometric Sensors for D_2O. *Chem* **2017**, *2*, 459–469.

(12) Park, S.-H.; Kwon, N.; Lee, J.-H.; Yoon, J.; Shin, I. Synthetic ratiometric fluorescent probes for detection of ions. *Chem. Soc. Rev.* **2020**, *49*, 143–179.

(13) Qi, Y.-L.; Li, Y.-Z.; Tan, M.-J.; Yuan, F.-F.; Murthy, N.; Duan, Y.-T.; Zhu, H.-L.; Yang, S.-Y. Recent advances in organic near-infrared ratiometric small-molecule fluorescent probes. *Coord. Chem. Rev.* **2023**, *486*, 215130.

(14) Shi, H.; Ma, X.; Zhao, Q.; Liu, B.; Qu, Q.; An, Z.; Zhao, Y.; Huang, W. Ultrasmall Phosphorescent Polymer Dots for Ratiometric Oxygen Sensing and Photodynamic Cancer Therapy. *Adv. Funct. Mater.* **2014**, *24*, 4823–4830.

(15) Huang, X.; Song, J.; Yung, B. C.; Huang, X.; Xiong, Y.; Chen, X. Ratiometric optical nanoprobes enable accurate molecular detection and imaging. *Chem. Soc. Rev.* **2018**, *47*, 2873–2920.

(16) Xiao, M.; Lai, W.; Man, T.; Chang, B.; Li, L.; Chandrasekaran, A. R.; Pei, H. Rationally Engineered Nucleic Acid Architectures for Biosensing Applications. *Chem. Rev.* **2019**, *119*, 11631–11717.

(17) Broza, Y. Y.; Zhou, X.; Yuan, M.; Qu, D.; Zheng, Y.; Vishinkin, R.; Khatib, M.; Wu, W.; Haick, H. Disease Detection with Molecular Biomarkers: From Chemistry of Body Fluids to Nature-Inspired Chemical Sensors. *Chem. Rev.* **2019**, *119*, 11761–11817.

(18) Tian, X.; Murfin, L. C.; Wu, L.; Lewis, S. E.; James, T. D. Fluorescent small organic probes for biosensing. *Chem. Sci.* **2021**, *12*, 3406–3426.

(19) Liu, L.; Wang, X.; Zhu, S.; Li, L. Different Surface Interactions between Fluorescent Conjugated Polymers and Biological Targets. *ACS Appl. Bio Maters.* **2021**, *4*, 1211–1220.

(20) Fang, H.; Chen, Y.; Jiang, Z.; He, W.; Guo, Z. Fluorescent Probes for Biological Species and Microenvironments: from Rational Design to Bioimaging Applications. *Acc. Chem. Res.* **2023**, *56*, 258–269.

(21) Mizuno, H.; Fukuhara, G. Solution-State Hydrostatic Pressure Chemistry: Application to Molecular, Supramolecular, Polymer, and Biological Systems. *Acc. Chem. Res.* **2022**, *55*, 1748–1762.

(22) Du, J.; Ma, Q.; Wang, B.; Sun, L.; Liu, L. Hydrogel fibers for wearable sensors and soft actuators. *iScience* **2023**, *26*, 106796.

(23) Beeren, S. R.; McTernan, C. T.; Schaufelberger, F. The mechanical bond in biological systems. *Chem* **2023**, *9*, 1378–1412.

(24) Ji, J.; Wei, X.; Wu, W.; Yang, C. Asymmetric Photoreactions in Supramolecular Assemblies. *Acc. Chem. Res.* doi: 10.1021/acs.accounts.3c00234.

(25) Sagara, Y.; Kato, T. Mechanically induced luminescence changes in molecular assemblies. *Nat. Chem.* **2009**, *1*, 605–610.

(26) Pucci, A.; Bizzarri, R.; Ruggeri, G. *Soft Matter* **2011**, *7*, 3689–3700.

(27) Xue, P.; Ding, J.; Wang, P.; Lu, R. Recent progress in the mechanochromism of phosphorescent organic molecules and metal complexes. *J. Mater. Chem. C* **2016**, *4*, 6688–6706.

(28) Meersman, F.; Dobson, C. M.; Heremans, K. Protein unfolding, amyloid fibril formation and configurational energy landscapes under high pressure conditions. *Chem. Soc. Rev.* **2006**, *35*, 908–917.

(29) Murthy, S. E.; Dubin, A. E.; Patapoutian, A. Piezo thrive under pressure: mechanically activated ion channels in health and disease. *Nat. Rev. Mol. Cell Biol.* **2017**, *18*, 771–783.

(30) Mohammed, D.; Versaevel, M.; Bruyère, C.; Alaimo, L.; Luciano, M.; Vercruysse, E.; Procès, A.; Gabriele, S. Innovative Tools for Mechanobiology: Unraveling Outside-In and Inside-Out Mechanotransduction. *Front. Bioeng. Biotechnol.* **2019**, *7*, 162–179.

(31) Bovey, F. A.; Yanari, S. S. Effect of Solvent Polarizability on the Ultra-Violet Spectral Shifts of Aromatic Compounds. *Nature* **1960**, *186*, 1042–1044.

(32) Johnson, P. C.; Offen, H. W. Effect of Pressure on Pyrene Excimer Fluorescence in Toluene. *J. Chem. Phys.* **1972**, *56*, 1638–1642.

(33) Weber, G.; Tanaka, F.; Okamoto, B. Y.; Drickamer, H. G. The Effect of Pressure on the Molecular Complex of Isoalloxazine and Adenine. *Proc. Nat. Acad. Sci. USA* **1974**, *71*, 1264–1266.

(34) Rollinson, A. M.; Drickamer, H. G. High Pressure Study of Luminescence from Intramolecular CT Compounds. *J. Chem. Phys.* **1980**, *73*, 5981–5996.

(35) Hara, K.; Yano, H. High-Pressure Study on Intramolecular Excimer Formation of 1,3-Di-1-pyrenylpropane in Various Solvents. *J. Am. Chem. Soc.* **1988**, *110*, 1911–1915.

(36) Hara, K.; Rettig, W. Effect of Pressure on the Fluorescence of TICT States in (*N,N*-Dimethylamino)benzonitrile and Its Related Compounds. *J. Phys. Chem.* **1992**, *96*, 8307–8309.

(37) Rettig, W.; Gilabert, E.; Rulliére, C. Pressure Dependence of Bicimer Formation in 4-Dimethylamino-4'-cyanostilbene and Model Compounds. *Chem. Phys. Lett.* **1994**, *229*, 127–133.

(38) Asano, T.; Furuta, H.; Sumi, H. "Two-Step" Mechanism in Single-Step Isomerizations. Kinetics in Highly Viscous Liquid Phase. *J. Am. Chem. Soc.* **1994**, *116*, 5545–5550.

(39) Hara, K.; Kometani, N.; Kajimoto, O. High-Pressure Studies on the Excited-State Intramolecular Charge Transfer of 4-(*N,N*-Dimethylamino)triphenylphosphine in Alcohols. *J. Phys. Chem.* **1996**, *100*, 1488–1493.

(40) Isaacs, N. S.; Nichols, P. J.; Raston, C. L.; Sandova, C. A.; Young, D. J. Solution volume studies of a deep cavity inclusion complex of C_{60}: [*p*-benzylcalix[5]arene $\subset$ C_{60}]. *Chem. Commun.* **1997**, 1839–1997.

(41) Ariga, K.; Terasaka, Y.; Sakai, D.; Tsuji, H.; Kikuchi, J. Piezoluminescence Based on Molecular Recognition by Dynamic Cavity Array of Steroid Cyclophanes at the Air-Water Interface. *J. Am. Chem. Soc.* **2000**, *122*, 7835–7836.

(42) Ruan, K.; Tian, S.; Lange, R.; Balny, C. Pressure Effects on Tryptophan and Its Derivatives. *Biochem. Biophys. Res. Commun.* **2000**, *269*, 681–686.

(43) Saudan, C.; Dunand, F. A.; Abou-Hamdan, A.; Bugnon, P.; Lye, P. G.; Lincoln, S. F.; Merbach, A. E. A Model for Sequential

Threading of α-Cyclodextrin onto a Guest: A Complete Thermodynamic and Kinetic Study in Water. *J. Am. Chem. Soc.* **2001**, *123*, 10290–10298.

(44) Ruloff, R.; Seelbach, U. P.; Merbach, A. E.; Klärner, F.-G. Molecular tweezers as synthetic receptors: the effect of pressure and temperature on the formation of host-guest complexes. *J. Phys. Org. Chem.* **2002**, *15*, 189–196.

(45) Hablot, D.; Ziessel, R.; Alamiry, M. A. H.; Bahraidah, E.; Harriman, A. Nanomechanical Properties of Molecular-Scale Bridges as Visualized by Intramolecular Electronic Energy Transfer. *Chem. Sci.* **2013**, *4*, 444–453.

(46) Suhina, T.; Weber, B.; Carpentier, C. E.; Lorincz, K.; Schall, P.; Bonn, D.; Brouwer, A. M. Fluorescence Microscopy Visualization of Contacts Between Objects. *Angew. Chem., Int. Ed.* **2015**, *54*, 3688–3691.

(47) Lee, R.; Howard, J. A. K.; Probert, M. R.; Steed, J. W. Structure of Organic Solids at Low Temperature and High Pressure. *Chem. Soc. Rev.* **2014**, *43*, 4300–4311.

(48) O'Bannon III, E. F.; Jenei, Z.; Cynn, H.; Lipp, M. J.; Jeffries, J. R. Contributed Review: Culet Diameter and the Achievable Pressure of a Diamond Anvil Cell: Implications for the Upper Pressure Limit of a Diamond Anvil Cell. *Rev. Sci. Instrum.* **2018**, *89*, 111501.

(49) Takeda, Y.; Mizuno, H.; Okada, Y.; Okazaki, M.; Minakata, S.; Penfold, T.; Fukuhara, G. *ChemPhotoChem* **2019**, *3*, 1203–1211.

(50) Nakasha, K.; Fukuhara, G. *ACS Appl. Polym. Maters.* **2020**, *2*, 2303–2310.

(51) Casier, R.; Duhamel, J. Effect of Like Charges on the Conformation and Internal Dynamics of Polypeptides Probed by Pyrene Excimer Fluorescence. *Macromolecules* **2020**, *53*, 5147–5157.

(52) Lee, S.; Winnik, M. A.; Cyclization Rates for Two Points in the Interior of a Polymer Chain. *Macromolecules* **1997**, *30*, 2633–2641.

(53) Thoma, J. L.; Duhamel, J.; Bertocchi, M. J.; Weiss, R. G. Long Range Polymer Chain Dynamics of Highly Flexible Polysiloxane in Solution Probed by Pyrene Excimer Fluorescence. *Polyms.* **2018**, *10*, 345.

(54) Wrona-Piotrowicz, A.; Zakrzewski, J.; Métivier, R.; Brosseau, A.; Makal, A.; Woźniak, K. Efficient synthesis of pyrene-1-carbothioamides and carboxamides. Tunable solid-state fluorescence of pyrene-1-carboxamides. *RSC Adv.* **2014**, *4*, 56003–56012.

(55) Mizuno, H.; Kitamatsu, M.; Imai, Y.; Fukuhara, G. Smart Fluorescence Materials that Are Controllable by Hydrostatic Pressure: Peptide-Pyrene Conjugates. *ChemPhotoChem* **2020**, *4*, 502–507.

(56) Nakabayashi, T.; Morikawa, T.; Ohta, N. Direct measurements of the electric-filed-induced change in fluorescence decay profile of pyrene doped in a polymer film. *Chem. Phys. Lett.* **2004**, *395*, 346–350.

(57) Myer, Y. P. The pH-Induced Helix-Coil Transition of Poly-L-lysine and Poly-L-glutamic Acid and the 238-mμ Dichroic Band. *Macromolecules* **1969**, *2*, 624–628.

(58) Isdale, J. D.; Easteal, A. J.; Woolf, L. A. Shear Viscosity of Methanol and Methanol + Water Mixtures Under Pressure. *Int. J. Thermophys.* **1985**, *6*, 439–450.

(59) Schmelzer, J. W. P.; Zanotto, E. D.; Fokin, V. M. Pressure dependence of viscosity. *J. Chem. Phys.* **2005**, *122*, 074511.

(60) Lee, H.-H.; Yamaguchi, H.; Fujimori, D.; Ohnishi, T.; Nishida, A.; Yamamoto, H. Synthesis and Conformation of Monodispersed Oligo(ε-L-Lisine)mers Studied by Cd and IR Spectroscopies. *Spectr. Lett.* **1995**, *28*, 177–190.

(61) Ito, S.; Ikeda, K.; Nakanishi, S.; Imai, Y.; Asami, M. Concentration-dependent circularly polarized luminescence (CPL) of chiral *N*,*N*'-dipyrenyldiamines: sign-inverted CPL switching between monomer and excimer regions under retention of the monomer emission for photoluminescence. *Chem. Commun.* **2017**, *53*, 6323–6326.

(62) Takaishi, K.; Iwachido, K.; Ema, T. Solvent-Induced Sign Inversion of Circularly Polarized Luminescence: Control of Excimer Chirality by Hydrogen Bonding. *J. Am. Chem. Soc.* **2020**, *142*, 1774–1779.

TOC